Table 4.1: Related work comparison among various Markov process-based models.

Reference	Imperfect Sensing	Continuous Sensing	Heteroge-nous SUs	Buffer Support	Retrial Policy	Effect of FAR
Kim and Shin [214]	✓	✗	✗	✗	✗	✗
El-Sherif and Liu [216]	✓	✗	✗	✓	✗	✗
Liao et al. [218]	✓	✓	✗	✗	✗	✗
Tang and Xie [221]; Tang et al. [220]	✓	✓	✗	✓	✗	✗
Suliman et al. [210]	✓	✓	✗	✗	✗	✓
Kalil et al. [225]; Balapuwaduge et al. [227]	✗	✗	✓	✓	✓	✗
Zhao et al. [226]; Hong et al. [228]	✗	✗	✗	✓	✓	✗
Zhao et al. [229]	✗	✗	✓	✓	✗	✗
Proposed model	✓	✓	✓	✓	✓	✓

in the higher termination rate of the SUs. On the other hand, some existing studies such as by Zhao et al. [224] and Kalil et al. [225], considered that instead of direct leaving, an interrupted SU is suspended to wait for future transmission in a buffer. However, this kind of definite suspension for retrial transmission (i.e. with probability 1), may cause a greater delay for the SU. It follows that the delay of SUs can be reduced to some extent by considering the suspension to wait in buffer with some retrial probability, as discussed by Zhao et al. [226].

In addition, the fact that emerging 5G networks are envisioned to comprise heterogeneous applications with different QoS thus, studies investigating CRNs with heterogeneous SUs exist. For instance, a spectrum sharing scheme with buffering for new as well as interrupted SUs supporting heterogeneous traffic was proposed by Hong et al. [228]. Further, Zhao [229] analyzed the queueing delay in CRN with heterogeneous services and channels, wherein the incoming heterogeneous traffic of SUs are inserted into the same queue in the arrival order. Later on, a queueing framework with channel assembling strategy was developed by Balapuwaduge et al. [227], introducing two separate queues for heterogeneous traffic of SUs. Further, to mitigate the effects of secondary call interruption in CRNs with heterogeneous traffic, different resource management mechanisms were evaluated and compared by Castellanos-Lopez et al. [230]. However, all of them assumed the spectrum sensing to be perfect which is an impractical scenario.

The main limitation according to the available literature is that all the discussed realistic elements and key factors are not modeled in a single work, which may affect the accuracy of the results. Table 4.1 summarizes the literature on some key Markov process-based analytical models, providing a comparison among them. In the table, the "✓" symbol indicates that the analytical model supports the corresponding feature while the "✗" symbol indicates that the analytical model does not support the corresponding feature. In the following section, we show the proposed analytical model in detail.

4.3 Network Scenario and Assumptions

In the proposed spectrum access strategy, the SUs are allowed to access the spectrum of PU opportunistically when it is free from PU communication. The licensed spectrum band of a CRN consists of $N \in \mathbb{Z}^+$ frequency channels and each channel is allocated to a specific PU. These channels are shared among PUs, RSUs and NRSUs, with PUs having higher priority over SUs. For presentation convenience, the term SU commonly represents both SUs. The user arrivals follow Poisson processes with rates λ_1, λ_2 and λ_3 and the service times are exponentially distributed with rates μ_1, μ_2 and μ_3 for the PU, RSU and NRSU, respectively.

The SUs perform spectrum sensing continuously along with data transmission as shown in Fig. 4.1. A newly arriving SU senses the whole PU channel with a bandwidth B for T_s units of time. To reduce SU's self-interference effect, a sufficient guard band subchannel is used i.e. B_G. Meanwhile, to determine the presence of a returning PU, the SU continuously monitors the PU channel utilizing bandwidth B_S and makes sensing decision every T_d units of time. In accordance, if an initiating SU finds an idle channel, it makes use of the channel and starts its data transmission over a bandwidth of $B - B_G - B_S$.

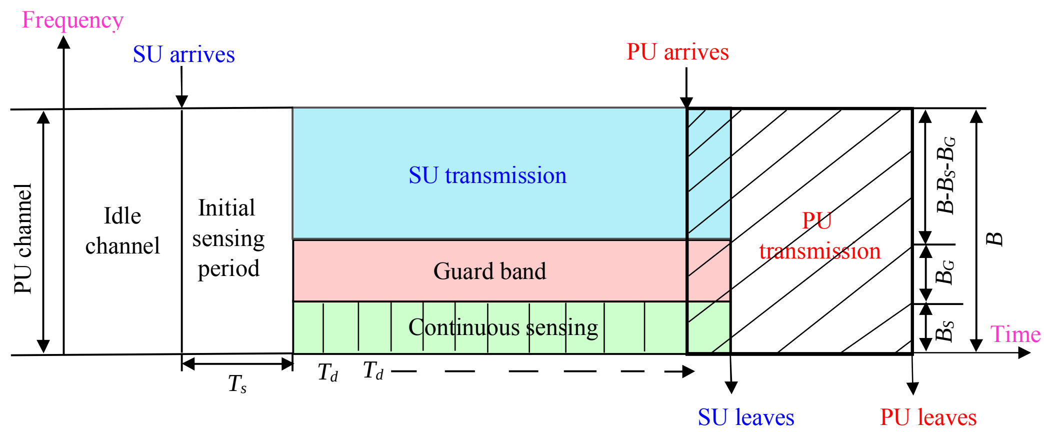

Figure 4.1: Continuous spectrum sensing and data transmission.

The prominent errors associated with the spectrum sensing process are the false alarms and mis-detections. Owing to unreliable sensing, each incoming SU correctly determines the presence of PU with probability P_{D1} and falsely classifies an idle channel as busy with probability P_{FA1}. Likewise, each ongoing SU correctly determines the presence of an arriving PU with probability P_{D2} and falsely classifies an idle channel as busy with probability P_{FA2}. The corresponding mis-detection probabilities for incoming and ongoing SUs are $P_{M1} = 1 - P_{D1}$ and $P_{M2} = 1 - P_{D2}$, respectively. At each spectrum sensing decision epoch T_d, a false alarm occurs with probability P_{FA2} and does not occur with probability $1 - P_{FA2}$, independent of the decision outcome of the last sensing period. The false alarm rate parameter, λ_{FAR} is the product of the decision rate and the false alarm probability. It follows that, λ_{FAR} is given by P_{FA2}/T_d. Moreover, to avoid the occurrence of too many false alarms for successful SU operation, we assume that the sensing interval T_d is short i.e. the decision rate given by $1/T_d$ is large and that the false alarm probability P_{FA2} is small. In consequence, as a limit of a shrinking Bernoulli process, the arrival process of false alarms can be approximated by a Poisson process with parameter λ_{FAR}, as suggested by Gallager [231]. The nomenclature is given in Table 4.2.

On the arrival of a new PU connection, the PU occupies one of the available free channels (if any). However, if the arriving PU finds all the channels occupied by other PUs, then it gets blocked. Also, if at least one channel is occupied by a SU, then the newly

Table 4.2: Nomenclature

Symbol	Description
N	Total number of channels in a cell.
Q_n	Buffer (NQ) capacity for non-real time secondary users' new calls.
Q_h	Buffer (PQ) capacity for non-real time secondary users' handoff calls.
λ_1	Arrival rate for primary users.
λ_2	Arrival rate for real time secondary users.
λ_3	Arrival rate for non-real time secondary users.
$1/\mu_1$	Average service time for primary users.
$1/\mu_2$	Average service time for real time secondary users.
$1/\mu_3$	Average service time for non-real time secondary users.
P_{D1}	Correct-detection probability for incoming secondary users.
P_{D2}	Correct-detection probability for ongoing secondary users.
P_{FA1}	False alarm probability for incoming secondary users.
P_{FA2}	False alarm probability for ongoing secondary users.
P_{M1}	Mis-detection probability for incoming secondary users.
P_{M2}	Mis-detection probability for ongoing secondary users.
λ_{FAR}	False alarm rate parameter.
p	Retrial probability for non-real time secondary users' handoff calls.
α	Probability of selection of a non-real time secondary user from the new buffer.

arriving PU interrupts the transmission of the SU and occupies the channel otherwise, it gets terminate in case of a collision with the SU.

To deal with heterogeneous traffic, we have deployed two separate queues. The queue named as NQ (new buffer) is utilized for new NRSU arrivals with maximum size Q_n while the queue named as PQ (handoff buffer) is used for interrupted NRSU services with maximum size Q_h. When all the channels are found to be occupied by SUs or sensed (correctly or incorrectly) as PU occupied, a newly arriving NRSU will occupy a waiting position in NQ whereas a new RSU service will get block. Further, in case of PU appearance, the ongoing SU should vacate its occupied channel and leave it to PU. To resume its communication, the interrupted SU performs a fast spectrum handoff to one of the other idle channels. However, if all the channels are found occupied, the interrupted

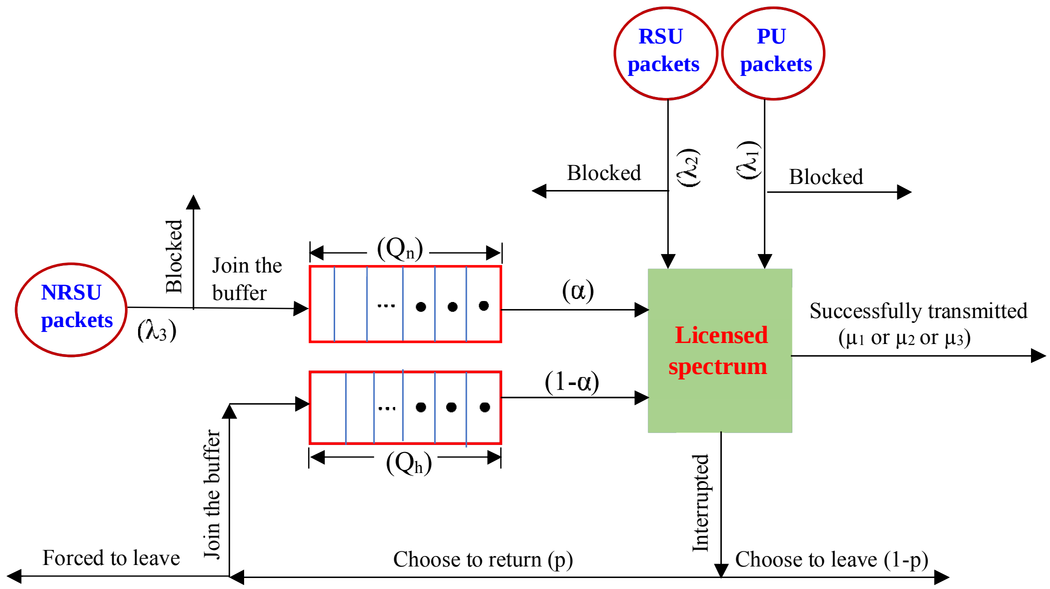

Figure 4.2: Illustration of the proposed queueing based spectrum access strategy with p-retry policy.

RSU services will get drop whereas according to the p-retry policy, the interrupted NRSU services will either be suspended to the buffer PQ with probability p $(0 < p < 1)$ for later retrial transmission, or will leave the system with probability $(1 - p)$ and gives up its transmission. Accordingly, if the interrupted NRSU services can be queued for later retrial transmission, the forced dropping probability of NRSU services can be reduced, however, at a cost of longer queueing delay. Therefore, for delay-sensitive applications like real-time traffic, it is better not to feed the interrupted RSU services.

In addition, we assume that the interrupted NRSU services have priority over the newly arriving NRSU services. The channels which become idle are allocated to the awaiting NRSUs in PQ and NQ buffer. The probability of selection of an NRSU service from NQ buffer is α $(0 < \alpha < 1)$, then the probability of its selection from PQ buffer is (1-α), in a way giving higher priority to interrupted NRSU services i.e. $\alpha < 0.5$. Moreover, it is assumed that in the case of collisions due to false alarms or mis-detections (between PU and SU), both colliding users withdraw from the system. Based on the above assumptions, we depict the proposed spectrum access strategy in Fig. 4.2.

4.4 Markov Chain Modeling

The system is modeled using a five-dimensional CTMC. At any instant, the system state is determined by $\boldsymbol{x} = (i, j, k, l, m)$ where i is the number of in-service PUs, j denotes the number of in-service RSUs, k denotes the number of in-service NRSUs, l represents the number of queued new NRSUs and m represents the number of queued interrupted (handoff) NRSUs. The corresponding set of feasible states, S in the CTMC model is given by

$$S = \{(i, j, k, l, m) \mid 0 \leq i \leq N, 0 \leq j \leq N, 0 \leq k \leq N, \\ 0 \leq i + j + k \leq N, 0 \leq l \leq Q_n, 0 \leq m \leq Q_h\}. \quad (4.1)$$

Because of the imperfect sensing, the number of PUs, NRSUs and RSUs will affect the channel searching results. In view of this, to accurately model CRN, the CTMC includes state-dependent transition rates by taking into account the number of users in the channel searching process. Each feasible state transition is associated to a given probability/rate.

Consider the number of idle channels in state $\boldsymbol{x} = (i, j, k, l, m)$ to be $r = N - i - j - k$. For the sequel, we define the indicator variable, θ as

$$\theta = \begin{cases} 0; & \text{if } l = 0 \\ 1; & \text{if } m = 0 \\ \alpha; & \text{if } l > 0 \text{ and } m > 0. \end{cases} \quad (4.2)$$

Since the number of states grows largely with the number of channels and buffer sizes in the system, the recursive approach is utilized to derive CTMC transition rates to describe a CRN with an arbitrary number of channels and buffer sizes. Function $f(.)$ is used to define the increase in number of SUs by 1. We have the recursion,

$$f(i, r) = \frac{r}{i + r}(1 - P_{FA1}) + \frac{r}{i + r} P_{FA1} f(i, r - 1) + \frac{i}{i + r} P_{D1} f(i - 1, r), \quad (4.3)$$

Table 4.3: Transitions from a generic state $\boldsymbol{x} = (i, j, k, l, m)$ upon PU events.

Destination State	Trans. rate	Conditions (Indicator variable)
$(i+1, j, k, l, m)$	$\alpha_1\lambda_1\left(\frac{N-i-j-k}{N-i}\right) + \alpha_2\lambda_1\frac{k}{N-i}P_{D2}f(i,r)$	$\alpha_1 = \begin{cases} 1\,; 0 < i+j+k < N, l=0, m=0 \\ 0;\ otherwise. \end{cases}$
	$+\,\alpha_3\lambda_1\frac{j}{N-i}P_{D2}f(i,r)$	$\alpha_2 = \begin{cases} 1; 0 < i+j+k < N, k>0, l=0, m=0 \\ 0;\ otherwise. \end{cases}$
		$\alpha_3 = \begin{cases} 1; 0 < i+j+k < N, j>0, l=0, m=0 \\ 0;\ otherwise. \end{cases}$
$(i+1, j, k-1, l, m)$	$\alpha_4\lambda_1\frac{k}{N-i}P_{D2}(1-f(i,r)-g(i,r))(1-p)$	$\alpha_4 = \begin{cases} 1; i+j+k=N, k>0, 0\le l\le Q_n, 0\le m\le Q_h \\ 0;\ otherwise. \end{cases}$
	$+\,\alpha_5\lambda_1\frac{k}{N-i}P_{D2}(1-f(i,r)-g(i,r))p$	$\alpha_5 = \begin{cases} 1; i+j+k=N, k>0, 0\le l\le Q_n, m=Q_h \\ 0;\ otherwise. \end{cases}$
$(i+1, j-1, k, l, m)$	$\alpha_6\lambda_1\frac{j}{N-i}P_{D2}(1-f(i,r)-g(i,r))$	$\alpha_6 = \begin{cases} 1; i+j+k=N, j>0, 0\le l\le Q_n, 0\le m\le Q_h \\ 0;\ otherwise. \end{cases}$
$(i+1, j, k-1, l, m+1)$	$\alpha_7\lambda_1\frac{k}{N-i}P_{D2}(1-f(i,r)-g(i,r))p$	$\alpha_7 = \begin{cases} 1; i+j+k=N, k>0, 0\le l\le Q_n, 0\le m< Q_h \\ 0;\ otherwise. \end{cases}$
$(i-1, j, k, l, m)$	$\alpha_8(i\mu_1+\lambda_2 g(i,r)+\lambda_3 g(i,r))$	$\alpha_8 = \begin{cases} 1;\ 0 < i+j+k\le N, i>0, l=0, m=0 \\ 0;\ otherwise. \end{cases}$
$(i-1, j, k+1, l-1, m)$	$\alpha_9\theta(i\mu_1+\lambda_2 g(i,r)+\lambda_3 g(i,r))$	$\alpha_9 = \begin{cases} 1;\ i+j+k-N, i>0, 0<l\le Q_n, 0\le m\le Q_h \\ 0;\ otherwise. \end{cases}$
$(i-1, j, k+1, l, m-1)$	$\alpha_{10}(1-\theta)(i\mu_1+\lambda_2 g(i,r)+\lambda_3 g(i,r))$	$\alpha_{10} = \begin{cases} 1;\ i+j+k=N, i>0, 0\le l\le Q_n; 0<m\le Q_h \\ 0;\ otherwise. \end{cases}$

For boundary values we get by induction,

$$f(0,r) = 1 - P_{FA1}^r, \tag{4.4}$$

$$f(i,1) = \frac{1}{i+1}(1-P_{FA1})\sum_{n=0}^{\infty} P_{D1}^i. \tag{4.5}$$

Also, we use the recursive function $g(.)$ to define the decrease in number of PUs by 1. We get the recursion,

$$g(i,r) = \frac{i}{i+r}P_{M1} + \frac{i}{i+r}P_{D1}g(i-1,r) + \frac{r}{i+r}P_{FA1}g(i,r-1). \tag{4.6}$$

Using the recursive approach then, the transitions from state $\boldsymbol{x} = (i, j, k, l, m)$ are described as follows and summarized in Tables 4.3 to 4.5.

- Transition to $(i+1, j, k, l, m)$. This transition happens if one of the following three events occur: Firstly, when a PU arrives on a free channel and occupies it. Secondly, when a PU arrives on a channel occupied by an NRSU. Therefore, the NRSU performs a spectrum handoff to another free channel. Thirdly, when a PU arrives on a channel occupied by an RSU, and the interrupted RSU performs a spectrum handoff to another free channel.

- Transition to $(i+1, j, k-1, l, m)$. This transition happens if one of the following two events occur: Firstly, when a PU arrives on a channel occupied by an NRSU, the interrupted NRSU doesn't find a free channel to perform handoff and leaves the system. Secondly, when this interrupted NRSU doesn't find a free channel to perform handoff, decides to queue in the PQ buffer but finds the buffer full. As a result, the NRSU drops.

- Transition to $(i+1, j-1, k, l, m)$. This transition occurs when a PU arrives on a channel occupied by an RSU but the interrupted RSU doesn't find a free channel to perform spectrum handoff. As a result, the RSU drops.

- Transition to $(i+1, j, k-1, l, m+1)$. This transition happens when a PU arrives on a channel occupied by an NRSU, the interrupted NRSU doesn't find a free channel and gets queued in the PQ buffer.

- Transition to $(i-1, j, k, l, m)$. This transition happens if both the buffers are empty and one of the following events occurs: Firstly, when one of the existing PUs completes its service. Secondly and thirdly, when a newly arriving RSU or a newly arriving NRSU ends up colliding with PU after channel searching on a channel already occupied by PU.

- Transition to $(i-1, j, k+1, l-1, m)$. This occurs when a PU completes its service or an arriving RSU ends up colliding with PU and then, the idle channel is allocated to the NRSU at the head of the new buffer. Likewise, in case if the idle channel is allocated to the NRSU at the head of the handoff buffer, transition to $(i-1, j, k+1, l, m-1)$ happens.

- Transition to $(i, j+1, k, l, m)$. This occurs if a newly arriving RSU occupies an idle channel.

Table 4.4: Transitions from a generic state $\boldsymbol{x} = (i, j, k, l, m)$ upon RSU events.

Destination State	Trans. rate	Conditions (Indicator variable)
$(i, j+1, k, l, m)$	$\beta_1 \lambda_2 f(i, r)$	$\beta_1 = \begin{cases} 1; \ 0 \leq i+j+k < N, l=0, m=0 \\ 0; \ otherwise. \end{cases}$
$(i, j-1, k, l, m)$	$\beta_2 \Big(j\mu_2 + \lambda_1 \frac{j}{N-i} P_{M2} + \lambda_1 \frac{j}{N-i} P_{D2} g(i, r) \Big)$	$\beta_2 = \begin{cases} 1; \ 0 < i+j+k \leq N, j>0, l=0, m=0 \\ 0; \ otherwise. \end{cases}$
	$+\beta_3 (j \lambda_{FAR} (1 - f(i, r) - g(i, r))$	$\beta_3 = \begin{cases} 1; \ i+j+k = N, j>0, l=0, m=0 \\ 0; \ otherwise. \end{cases}$
$(i, j-1, k+1, l-1, m)$	$\beta_4 \theta \Big(j\mu_2 + \lambda_1 \frac{j}{N-i} P_{M2} + \lambda_1 \frac{j}{N-i} P_{D2} g(i, r)$ $+ j\lambda_{FAR} (1 - f(i, r) - g(i, r) \Big)$	$\beta_4 = \begin{cases} 1; \ i+j+k = N, j>0, 0 < l \leq Q_n, 0 \leq m \leq Q_h \\ 0; \ otherwise. \end{cases}$
$(i, j-1, k+1, l, m-1)$	$\beta_5 (1-\theta) \Big(j\mu_2 + \lambda_1 \frac{j}{N-i} P_{M2} + \lambda_1 \frac{j}{N-i} P_{D2} g(i, r)$ $+ j\lambda_{FAR} (1 - f(i, r) - g(i, r) \Big)$	$\beta_5 = \begin{cases} 1; \ i+j+k = N, j>0, 0 \leq l \leq Q_n, 0 < m \leq Q_h \\ 0; \ otherwise. \end{cases}$
$(i-1, j-1, k, l, m)$	$\beta_6 j \lambda_{FAR} g(i, r)$	$\beta_6 = \begin{cases} 1; \ 0 < i+j+k \leq N, i>0, j>0, l=0, m=0 \\ 0; \ otherwise. \end{cases}$
$(i-1, j-1, k+2, l-1, m-1)$	$\beta_7 \theta (1-\theta) j \lambda_{FAR} g(i, r)$	$\beta_7 = \begin{cases} 1; \ i+j+k = N, i>0, j>0, 0 < l < Q_n, 0 < m < Q_h \\ 0; \ otherwise. \end{cases}$
$(i-1, j-1, k+2, l-2, m)$	$\beta_8 \theta^2 j \lambda_{FAR} g(i, r)$	$\beta_8 = \begin{cases} 1; \ i+j+k = N, i>0, j>0, 1 < l \leq Q_n, 0 \leq m \leq Q_h \\ 0; \ otherwise. \end{cases}$
$(i-1, j-1, k+2, l, m-2)$	$\beta_9 (1-\theta)^2 j \lambda_{FAR} g(i, r)$	$\beta_9 = \begin{cases} 1; \ i+j+k = N, i>0, j>0, 0 < l < Q_n, 1 < m < Q_h \\ 0; \ otherwise. \end{cases}$

- Transition to $(i, j-1, k, l, m)$. This occurs when both the buffers are empty and one of the following events occur. Firstly, when an RSU completes its service and departs. Secondly, if after a mis-detection, the ongoing RSU ends up colliding with an arriving PU. Thirdly, when upon arrival of a PU, the ongoing RSU makes correct detection and vacates the channel but ends up colliding with another PU. Fourthly, if after the occurrence of FAR, the RSU neither finds a free channel nor gets collide and leaves the system.

  Furthermore, under all these cases, when at least one of the buffers is non empty, transition to $(i, j-1, k+1, l-1, m)$ or $(i, j-1, k+1, l, m-1)$ occurs accordingly.

  Similarly, when instead of RSU, NRSU undergoes the above events, the transition occurs to $(i, j, k-1, l, m)$ including the fourth event in case the NRSU chooses to leave the system and both the buffers are empty. Otherwise, if at least one of the buffers is non-empty, the transition happens to $(i, j, k, l-1, m)$ or $(i, j, k, l, m-1)$ respectively, including the fourth event when the NRSU chooses to leave the system voluntarily or when chooses to join the buffer but finds the buffer full.

- Transition to $(i-1, j-1, k, l, m)$. This transition happens if, after the occurrence

Table 4.5: Transitions from a generic state $\boldsymbol{x} = (i, j, k, l, m)$ upon NRSU events.

Destination State	Trans. rate	Conditions (Indicator variable)
$(i, j, k+1, l, m)$	$\gamma_1 \lambda_3 f(i, r)$	$\gamma_1 = \begin{cases} 1; \ 0 \le i+j+k < N, l=0, m=0 \\ 0; \ otherwise. \end{cases}$
$(i, j, k, l+1, m)$	$\gamma_2 \lambda_3$	$\gamma_2 = \begin{cases} 1; \ i+j+k = N, 0 \le l < Q_n, 0 \le m \le Q_h \\ 0; \ otherwise. \end{cases}$
$(i, j, k-1, l, m)$	$\gamma_3 \Big(k\mu_3 + \lambda_1 \frac{k}{N-i} P_{M2} + \lambda_1 \frac{k}{N-i} P_{D2} g(i, r) \Big)$	$\gamma_3 = \begin{cases} 1; \ i+j+k \le N, k > 0, l=0, m=0 \\ 0; \ otherwise. \end{cases}$
	$+\gamma_4 (k\lambda_{FAR}(1 - f(i, r) - g(i, r)(1-p))$	$\gamma_4 = \begin{cases} 1; \ i+j+k = N, k > 0, l=0, m=0 \\ 0; \ otherwise. \end{cases}$
$(i, j, k, l-1, m)$	$\gamma_5 \theta \Big(k\mu_3 + \lambda_1 \frac{k}{N-i} P_{M2} + \lambda_1 \frac{k}{N-i} P_{D2} g(i, r)$	$\gamma_5 = \begin{cases} 1; \ i+j+k = N, k > 0, 0 < l \le Q_n, 0 \le m \le Q_h \\ 0; \ otherwise. \end{cases}$
	$+k\lambda_{FAR}(1 - f(i, r) - g(i, r))(1-p) \Big)$	
	$+\gamma_6 \theta k\lambda_{FAR}(1 - f(i, r) - g(i, r))p$	$\gamma_6 = \begin{cases} 1; \ i+j+k = N, k > 0, 0 < l \le Q_n, m = Q_h \\ 0; \ otherwise. \end{cases}$
$(i, j, k-1, l, m+1)$	$\gamma_7 k\lambda_{FAR}(1 - f(i, r) - g(i, r))p$	$\gamma_7 = \begin{cases} 1; \ i+j+k = N, k > 0, l=0, m=0 \\ 0; \ otherwise. \end{cases}$
$(i, j, k, l-1, m+1)$	$\gamma_8 \theta k\lambda_{FAR}(1 - f(i, r) - g(i, r))p$	$\gamma_8 = \begin{cases} 1; \ i+j+k = N, k > 0, 0 < l \le Q_n, 0 \le m < Q_h \\ 0; \ otherwise. \end{cases}$
$(i, j, k, l, m-1)$	$\gamma_9 (1-\theta) \Big(k\mu_3 + \lambda_1 \frac{k}{N-i} P_{M2} + \lambda_1 \frac{k}{N-i} P_{D2} g(i, r)$	$\gamma_9 = \begin{cases} 1; \ i+j+k = N, k > 0, 0 \le l \le Q_n, 0 < m \le Q_h \\ 0; \ otherwise. \end{cases}$
	$+k\lambda_{FAR}(1 - f(i, r) - g(i, r))(1-p) \Big)$	
	$+\gamma_{10} (1-\theta) k\lambda_{FAR}(1 - f(i, r) - g(i, r))p$	$\gamma_{10} = \begin{cases} 1; \ i+j+k = N, k > 0, 0 \le l \le Q_n, m = Q_h \\ 0; \ otherwise. \end{cases}$
$(i-1, j, k-1, l, m)$	$\gamma_{11} k\lambda_{FAR} g(i, r)$	$\gamma_{11} = \begin{cases} 1; \ 0 < i+j+k \le N, i > 0, k > 0, l=0, m=0 \\ 0; \ otherwise. \end{cases}$
$(i-1, j, k+1, l-1, m-1)$	$\gamma_{12} \theta (1-\theta) k\lambda_{FAR} g(i, r)$	$\gamma_{12} = \begin{cases} 1; \ i+j+k = N, i > 0, k > 0, 0 < l \le Q_n, 0 < m \le Q_h \\ 0; \ otherwise. \end{cases}$
$(i-1, j, k+1, l-2, m)$	$\gamma_{13} \theta^2 k\lambda_{FAR} g(i, r)$	$\gamma_{12} = \begin{cases} 1; \ i+j+k = N, i > 0, k > 0, 1 < l \le Q_n, 0 \le m \le Q_h \\ 0; \ otherwise. \end{cases}$
$(i-1, j, k+1, l, m-2)$	$\gamma_{14} (1-\theta)^2 k\lambda_{FAR} g(i, r)$	$\gamma_{14} = \begin{cases} 1; \ i+j+k = N, i > 0, k > 0, 0 \le l \le Q_n, 1 < m \le Q_h \\ 0; \ otherwise. \end{cases}$

of false alarm, the RSU ends up owing to a collision with PU and both the buffers are empty.

Furthermore, if at least one of the buffers is non-empty then the two idle channels are allocated to the awaiting NRSUs in their respective buffers and consequently, transition happens to state $(i-1, j-1, k+2, l-1, m-1)$, $(i-1, j-1, k+2, l-2, m)$ or $(i-1, j-1, k+2, l, m-2)$. Also, in case when an NRSU undergoes the aforementioned events, the transition happens to $(i-1, j, k-1, l, m)$, $(i-1, j, k+1, l-1, m-1)$, $(i-1, j, k+1, l-2, m)$ or $(i-1, j, k+1, l, m-2)$ accordingly.

- Transition to $(i, j, k+1, l, m)$. This transition occurs if a newly arriving NRSU occupies a free channel.

- Transition to $(i, j, k, l+1, m)$. This happens when an NRSU arrives, finds all the channels occupied and gets queued in the new buffer.

- Transition to $(i, j, k-1, l, m+1)$. This occurs if after the occurrence of false alarm, the NRSU gets queued in the handoff buffer and both the buffers are empty.

  Furthermore, if the corresponding idle channel is allocated to the NRSU at the head of the new buffer, the transition occurs to $(i, j, k, l-1, m+1)$.

4.5 Performance Metrics

Based on the aforementioned analysis, we can obtain the transition rates between any two states of the considered five-dimensional CTMC, and thereby can formulate the state transition rate matrix, Q. Let $\pi(\boldsymbol{x})$ denote the steady-state probability of being in state $\boldsymbol{x}$. Accordingly, the steady-state probability vector Π, which is constituted by the stationary probabilities, $\pi(\boldsymbol{x})$ can be determined using the balance equations and the normalizing equation, given by

$$\Pi Q = 0, \sum_{\boldsymbol{x} \in S} \pi(\boldsymbol{x}) = 1.$$

When N, Q_n, Q_h are large, finding a solution to the corresponding balance equations gets complicated as the large number of states combined with the channel searching process would make it not trivial to derive the CTMC transition rates. The utilized recursive approach alleviates such problem. For CTMCs with very large number of states, which demands for higher memory and processing time, some approximation solutions with reduced number of channel states have been reported by Ciardo et al. [232]. However, the results presented in this chapter are obtained utilizing the exact full CTMC. Moreover, when the number of channels is very large, to overcome the problem of inefficiency, we can utilize approximate solutions of large CTMCs in Ciardo et al. [232]. Accordingly, in order to evaluate the performance of CRN, we derive different performance measures that are relevant to analyze the communication QoS, and are obtained as follows (please refer Tables 4.3 to 4.5 for conditions on indicator variables).

A. Blocking Probability

An incoming RSU gets blocked if upon its arrival all the channels are occupied. In such a case, the RSU blocking probability, BP_{RU}, can be written as follows

$$BP_{RU} = \sum_{i=0}^{N}\sum_{j=0}^{N-i}\sum_{l=0}^{Q_n}\sum_{m=0}^{Q_h} \pi_{(i,j,N-i-j,l,m)}. \tag{4.7}$$

Furthermore, an incoming NRSU will be blocked if there is no idle channel to commence the service and the buffer PQ is fully occupied. Therefore, the blocking probability, BP_{NRU}, is given by

$$BP_{NRU} = \sum_{i=0}^{N}\sum_{j=0}^{N-i}\sum_{m=0}^{Q_h} \pi_{(i,j,N-i-j,Q_n,m)}. \tag{4.8}$$

Contrarily, a PU only gets blocked when all the channels are occupied by PUs. Thus,

$$BP_{PU} = \sum_{l=0}^{Q_n}\sum_{m=0}^{Q_h} \pi_{(N,0,0,l,m)}. \tag{4.9}$$

B. Forced Termination Probability

As described by Suliman et al. [233], we use the term forced termination probability to refer to the probability that a call which has not been blocked initially, is terminated due to collisions because of the sensing errors i.e. mis-detections or false alarms. The forced termination probability of PUs, FTP_{PU}, can be expressed as ratio of mean forced termination rate of PUs to the mean admitted PU rate, $\lambda_1^* = \lambda_1(1 - BP_{PU})$. Correspondingly, the forced termination probability of PUs is given by

$$FTP_{PU} = \frac{\sum_{\boldsymbol{x}\in S}\Big(\Phi_1 + \Phi_2 + \Phi_3 + \Phi_4\Big)\pi(\boldsymbol{x})}{\lambda_1(1 - BP_{PU})}. \tag{4.10}$$

Similarly, the forced termination probabilities of RSUs, FTP_{RU} and NRSUs, FTP_{NRU} can be calculated as

$$FTP_{RU} = \frac{\sum_{\boldsymbol{x}\in S}\Big(\Phi_1 + \Phi_3\Big)\pi(\boldsymbol{x})}{\lambda_2(1 - BP_{RU})}, \tag{4.11}$$

$$FTP_{NRU} = \frac{\sum\limits_{\boldsymbol{x}\in S}\Big(\Phi_2 + \Phi_4\Big)\pi(\boldsymbol{x})}{\lambda_3(1 - BP_{NRU})}, \tag{4.12}$$

where

$$\Phi_1 = \big(\alpha_8 + \alpha_9\theta + \alpha_{10}(1-\theta)\big)\lambda_2 g(i,r), \tag{4.13}$$

$$\Phi_2 = \big(\alpha_8 + \alpha_9\theta + \alpha_{10}(1-\theta)\big)\lambda_3 g(i,r), \tag{4.14}$$

$$\begin{aligned}\Phi_3 = \lambda_1 \tfrac{j}{N-i}\big(\beta_2 + \beta_5(1-\theta)\big)\big(P_{M2} + P_{D2}g(i,r)\big)\\ +\big(\beta_6 + \beta_7\theta(1-\theta) + \beta_8\theta^2\\ +\beta_9(1-\theta)^2\big)\big(j\lambda_{FAR}g(i,r)\big),\end{aligned} \tag{4.15}$$

$$\begin{aligned}\Phi_4 = \lambda_1 \tfrac{k}{N-i}\big(\gamma_3 + \gamma_5\theta + \gamma_9(1-\theta)\big)\big(P_{M2} + P_{D2}g(i,r)\big)\\ +\big(\gamma_{11} + \gamma_{13}\theta(1-\theta) + \gamma_{13}\theta^2\\ +\gamma_{14}(1-\theta)^2\big)\big(k\lambda_{FAR}g(i,r)\big).\end{aligned} \tag{4.16}$$

C. Dropping Probability

A forced dropping of an RSU occurs when an interrupted RSU cannot find a free channel to handoff its call. In such a case, the forced dropping probability of RSU, FDP_{RU}, is given as follows

$$FDP_{RU} = \frac{\sum\limits_{\boldsymbol{x}\in S}\Big(A_1 + A_2\Big)\pi(\boldsymbol{x})}{\lambda_2^*(1 - FTP_{RU})}, \tag{4.17}$$

where

$$A_1 = \alpha_6\lambda_1\frac{j}{N-i}P_{D2}\big(1 - f(i,r) - g(i,r)\big), \tag{4.18}$$

$$A_2 = \big(\beta_3 + \beta_4\theta + \beta_5(1-\theta)\big)\big(j\lambda_{FAR}(1 - f(i,r) - g(i,r)\big). \tag{4.19}$$

Likewise, the forced dropping probability of NRSU, FDP_{NRU}, can be expressed as the total NRSU forced dropping rate divided by the total NRSU connection rate. When an interrupted NRSU ends searching without finding any other idle channel to handoff. In addition, the interrupted NRSU decides to return to the buffer PQ for later retrial transmission but finds the buffer full, then the NRSU has to drop its communication before its service is finished. Therefore,

$$FDP_{NRU} = \frac{\sum_{\boldsymbol{x} \in S} \Big(B_1 + B_2\Big)\pi(\boldsymbol{x})}{\lambda_3^*(1 - FTP_{NRU})}, \tag{4.20}$$

where

$$B_1 = \alpha_5 \lambda_1 \frac{k}{N-i} P_{D2}\big(1 - f(i,r) - g(i,r)\big)p, \tag{4.21}$$

$$B_2 = \big(\gamma_6\theta + \gamma_{10}(1-\theta)\big)\big(k\lambda_{FAR}(1 - f(i,r) - g(i,r)\big)p. \tag{4.22}$$

On the other hand, some interrupted NRSUs when ends the searching process without finding a new idle channel to handoff, will give up their transmissions and leave the system voluntarily. In this instance, we define the self dropping probability of NRSU, SDP_{NRU}, as follows

$$SDP_{NRU} = \frac{\sum_{\boldsymbol{x} \in S} \Big(C_1 + C_2\Big)\pi(\boldsymbol{x})}{\lambda_3^*(1 - FTP_{NRU})}, \tag{4.23}$$

where

$$C_1 = \alpha_4 \lambda_1 \frac{k}{N-i} P_{D2}\big(1 - f(i,r) - g(i,r)\big)(1-p), \tag{4.24}$$

$$C_2 = \big(\gamma_4 + \gamma_5\theta + \gamma_9(1-\theta)\big)\big(k\lambda_{FAR}(1 - f(i,r) - g(i,r)\big)(1-p). \tag{4.25}$$

D. Throughput

According to Kalil et al. [234], the throughput, T can be defined as the product of the number of successful SU connections per unit time and the service time per completed connection. Thus, the throughput of RSUs, T_{RU} and of NRSUs, T_{NRU} can be written as follows

$$T_{RU} = \lambda_2(1 - BP_{RU})(1 - FTP_{RU})^2(1 - FDP_{RU})^2\mu_2^{-1}, \tag{4.26}$$

$$T_{NRU} = \lambda_3(1 - BP_{NRU})(1 - FTP_{RU})^2(1 - FDPRU)^2(1 - SDPRU)^2\mu_3^{-1}. \tag{4.27}$$

E. Spectrum Utilization

In our analysis, we calculate the spectrum utilization of the system as the average number of utilized channels over the total number of channels available. Thus, the spectrum utilization of the CRN, U_{CRN}, can be expressed as

$$U_{CRN} = \frac{1}{N} \sum_{\boldsymbol{x} \in S} (i + j + k)\pi(\boldsymbol{x}). \tag{4.28}$$

4.6 Numerical Results and Discussion

The numerical results used to evaluate the performance of the proposed spectrum access strategy are presented below. The default values of the network configuration are $N = 6, P_{F1} = 0.15, P_{D1} = 0.75, \lambda_{FAR} = 10, P_{D2} = 0.95, \alpha = 0.2, \lambda_1 = 20, \lambda_2 = 15, \lambda_3 = 15, \mu_1 = \mu_2 = \mu_3 = 4, p = 0.7, Q_h = 2, Q_n = 4$, unless otherwise stated.

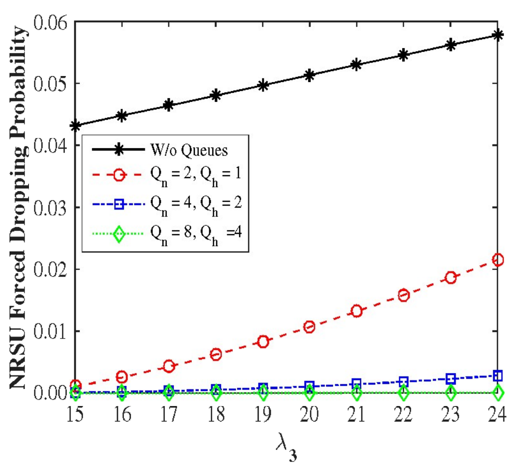

Figure 4.3: NRSU forced dropping probability as a function of NRSU arrival rate for different buffer sizes.

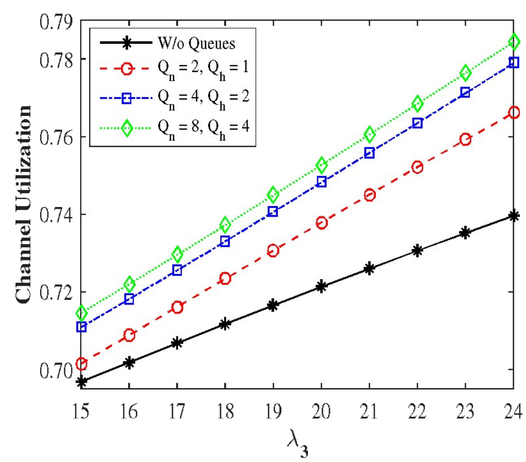

Figure 4.4: Spectrum utilization as a function of NRSU arrival rate for different buffer sizes.

Fig. 4.3 plots the forced dropping probability of NRSU with different values of buffer sizes. Intuitively with a higher NRSU arrival rate, the forced dropping probability of NRSUs increases, including the system without queues. From this figure, we observe that when queues are integrated the forced dropping probability of NRSUs gets reduce significantly. The result highlights that the increase in the size of handoff buffer has a more significant impact on the forced dropping probability of NRSUs. The reason is that the would-be-dropped NRSUs are not rejected but instead queued in the buffer (with probability p) in order to provide channel access when available. Also, it is seen that since a larger queue size allows to store more users' requests thus, results in lower forced dropping probability of NRSUs.

The spectrum utilization as a function of NRSU arrival rate, λ_3 is illustrated in Fig. 4.4. We observe that spectrum utilization is improved using our proposed queueing based strategy. When the scheme is evaluated without queues, it shows lower values compared to those with queues. Moreover, with higher λ_3, the improvement of spectrum utilization is more significant.

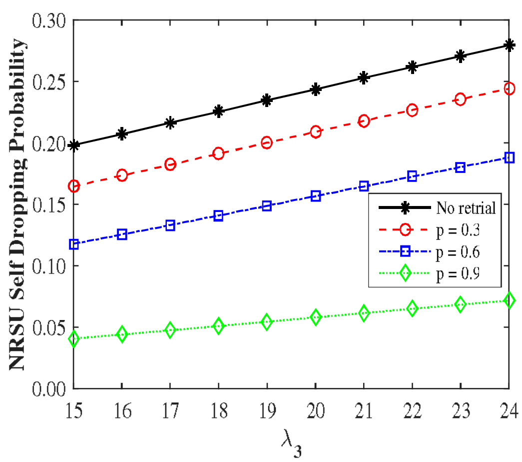

Figure 4.5: NRSU self dropping probability as a function of NRSU arrival rate for different retrial probabilities.

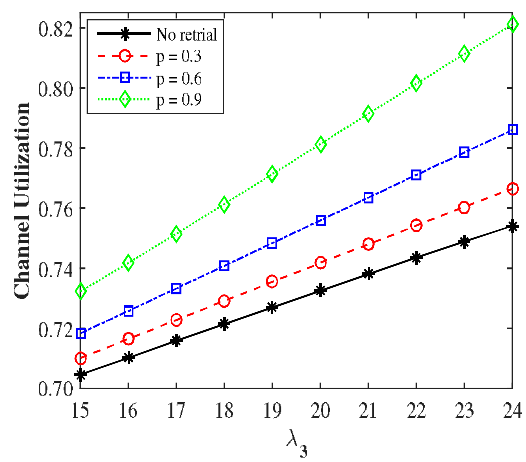

Figure 4.6: Spectrum utilization as a function of NRSU arrival rate for different retrial probabilities.

To further improve spectrum utilization, it is required to reduce the time period for channels being in idle state. It can be seen that the larger queue size can meet this requirement as more NRSUs' requests are allowed to accommodate in the queues. The self dropping probability of NRSU for different retrial probabilities, p is plotted in Fig. 4.5 as λ_3 varies. We observe that with higher active NRSUs, it is less likely for an interrupted NRSU to handoff to an idle channel, resulting in higher self dropping probability. As shown in the figure, the self dropping probability of NRSU decreases using the proposed spectrum access strategy with p-retry policy in contrast with the strategy without any retrial transmission. When using retry policy, the interrupted users due to insufficient channels instead of being dropped are allowed to queue in the buffer for later retrial transmission. This results in lower self dropping probability. Also, the larger the retrial probability is, the lesser are the number of interrupted NRSUs (voluntarily) getting dropped will be, so the self dropping probability of NRSU gets significantly reduced further.

Fig. 4.6 shows the effect of different retrial probabilities on spectrum utilization. We find improvement in spectrum utilization utilizing the proposed retry policy. With higher λ_3, the improvement is more significant. Since employing the retry policy, allows the would be dropped NRSUs to queue in the handoff buffer. Thus, when a channel becomes idle, it more likely to be utilized by an NRSU. Again, with larger retrial probability, greater number of interrupted NRSUs joins the buffer for retrial transmission. This reduces the time period for which channels remain in idle state, thus resulting in significant improvement of spectrum utilization.

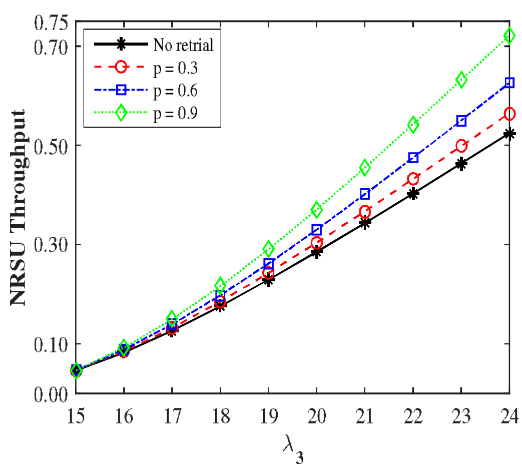

Figure 4.7: NRSU throughput as a function of NRSU arrival rate for different retrial probabilities.

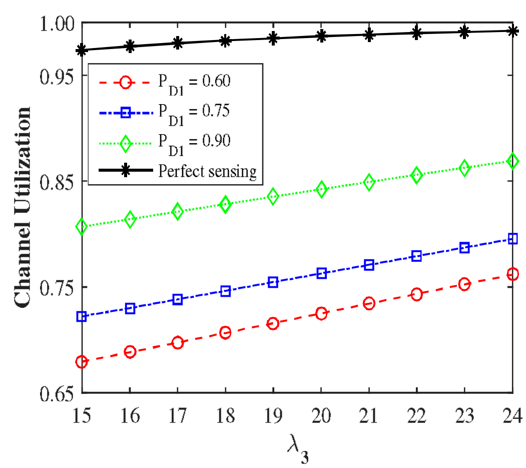

Figure 4.8: Spectrum utilization as a function of NRSU arrival rate for different correct-detection probabilities.

Further, Fig. 4.7 shows that the access retrial phenomenon given to NRSUs significantly improves the performance of the network in terms of the throughput of NRSUs, especially at high load conditions. Moreover, as the probability of retrial transmission increases, the number of NRSUs returning to the buffer increases. This results in more NRSUs to be transmitted and thus leads to higher throughput.

We show the effect of correct-detection probabilities, P_{D1} on spectrum utilization in Fig. 4.8 with varying λ_3. It can be observed that under perfect sensing, the licensed spectrum is better utilized. This is because in such cases, all unoccupied PUs' channels can be opportunistically utilized by SUs. On the other hand, we observe that the utilization of spectrum gets severely reduced after imposing the impact of sensing errors. The figure also highlights that the improved detection capability of SUs results in improvement of spectrum utilization significantly.

Fig. 4.9 depicts the effect of λ_3 on throughput of NRSUs with different configurations of P_{D1}. With perfect sensing, a SU is able to correctly classify all the unoccupied channels and the presence of PUs, therefore gives higher throughput. Further, it is apparent that the throughput of NRSU is greatly affected by the imperfect spectrum sensing. Due to the increase of P_{D1}, a transmission collision from imperfect spectrum sensing occurs seldom. As a result, NRSU obtains more opportunities for transmission, leading to higher throughput.

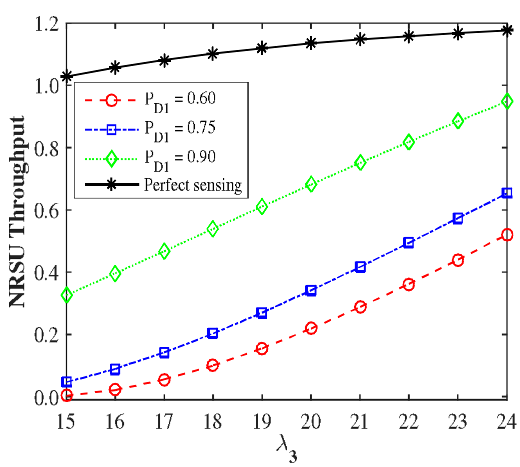

Figure 4.9: NRSU throughput as a function of NRSU arrival rate for different correct-detection probabilities.

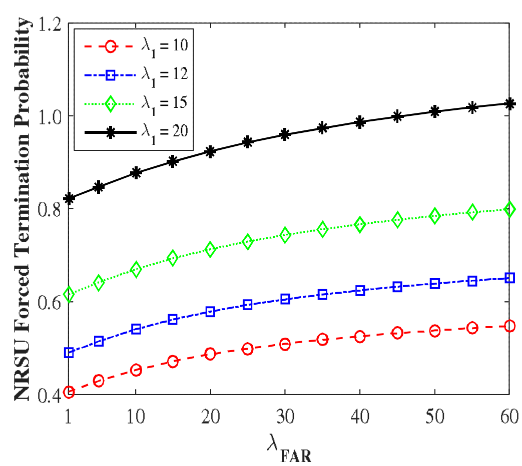

Figure 4.10: NRSU forced termination probability as a function of λ_{FAR} for different PU arrival rates.

In Fig. 4.10, the effect of false alarm rate, λ_{FAR} on the forced termination probability of NRSU is demonstrated. It can be seen that high λ_{FAR} degrades the NRSU performance. The degradation in NRSU performance can be explained by the fact that when λ_{FAR} is high, SUs increasingly initiate the unnecessary spectrum handoff process, leading to increment in NRSU termination probability. Moreover, the figure also indicates that the forced termination probability increases with a higher arrival rate of PUs. This is because, with a high primary arrival rate, most of the channels will be occupied by PUs, thus increasing the possibility of collisions with interrupted NRSUs.

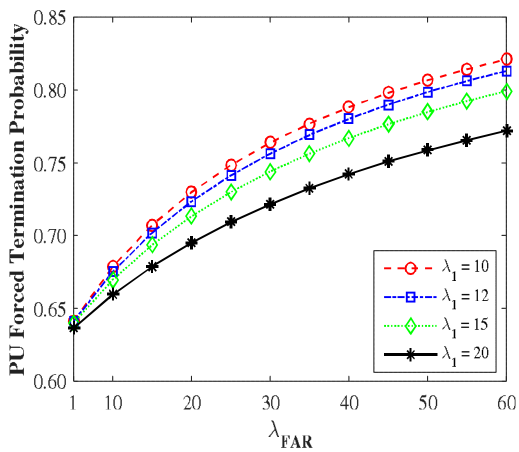

Figure 4.11: PU forced termination probability as a function of λ_{FAR} for different arrival rates of PU.

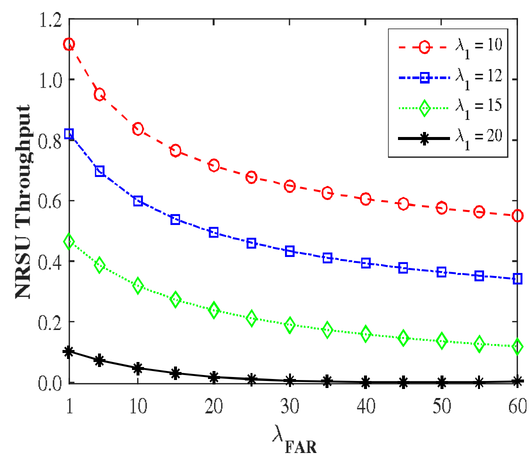

Figure 4.12: NRSU throughput as a function of λ_{FAR} for different arrival rates of PU.

In Fig. 4.11, we investigate the effect of λ_{FAR} on the forced termination probability of PU for different values of PU arrival rate. We observe that high λ_{FAR} leads to poor PU performance. This is because an increase in the number of occurrences of false alarms increases the proportion of SUs colliding with PUs, leading to higher primary call terminations. However, with high primary arrival, most of the channels are occupied by PUs. This lessens the SUs residing in the system to be interrupted by newly arriving PUs, resulting in a lower probability of collisions with PUs. Thereby, decreasing the forced termination probability of PUs.

We show the effect of λ_{FAR} on the throughput of NRSU in Fig. 4.12. It can be observed that increasing λ_{FAR} has a negative impact on NRSU performance in terms of throughput. As λ_{FAR} increases, a growing number of NRSUs initiate handoff process and gets terminated or dropped in case of collision or no free channel available. This indicates that NRSUs do not complete their service when λ_{FAR} is high and therefore, the throughput decreases. Also, at high primary arrival rate since the channels are more often occupied by PUs, it reduces the opportunities for NRSUs to access the spectrum and thus, results in lower throughput.

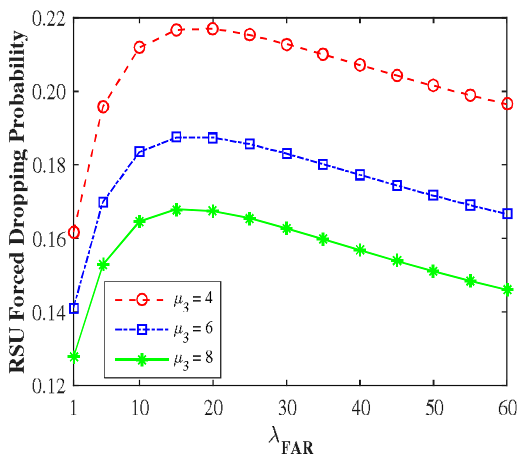

Figure 4.13: RSU forced dropping probability as a function of λ_{FAR} for different NRSU service rates.

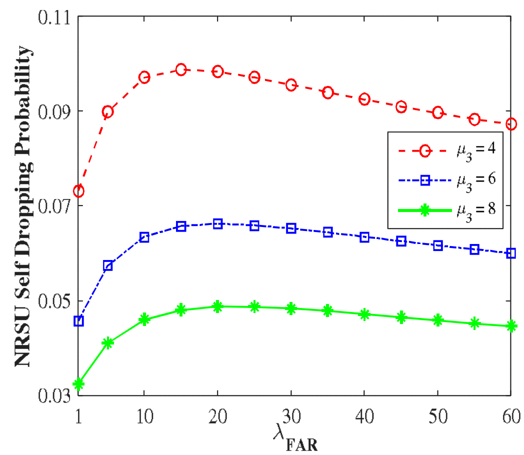

Figure 4.14: NRSU self dropping probability as a function of λ_{FAR} for different NRSU service rates.

Further, in Fig. 4.13, we measure the impact of λ_{FAR} on forced dropping probability of RSU for different service rates of NRSUs. It can be observed that there are peak values in the curves. The following explanation is related to this behavior. On one hand, when λ_{FAR} is relatively low, RSU forced dropping probability increases until it reaches the peak value and then starts to decline. The deterioration in RSU performance can be explained by the fact that as λ_{FAR} increases, unnecessary spectrum handoff increases, forcing RSUs to vacate and search for available channels to resume its communication. If they cannot find any other free channel, they get drop and thereby increases forced dropping probability. On the other hand, with high values of λ_{FAR} (and consequently high P_{D2}), the dropping probability gets reduce due to the improvement in the detection operation. Besides, we observe that diminishing the NRSU service duration, frees up its channels faster, enabling less RSU dropping events. Consequently, it enables a trade-off between λ_{FAR} and service time than can be tuned according to the different QoS requirements of the secondary users. The same effect of λ_{FAR} for increasing service rate of NRSU applies to the self dropping probability of NRSU as shown in Fig. 4.14.

4.7 Chapter Summary

The key emphasis of this chapter is to introduce and explore the concept of imperfect continuous spectrum sensing for heterogeneous traffic in CRNs. A joint design of spectrum sensing and spectrum access mechanisms is proposed and analyzed. More specifically, we have investigated a queue-based spectrum access strategy with p-retry policy for multi-channel CRNs. In subsequence, an analytical framework is developed to analyze the proposed strategy under realistic network operating conditions. The proposed strategy not only examines the effect of sensing errors by incoming SUs but also takes into account the mis-detection and false alarm probabilities by ongoing SUs. The effect of false alarm rates, λ_{FARs} is studied on the operation of CRNs. We have then evaluated performance of the system in terms of different performance metrics, including primary and secondary forced termination probabilities, dropping probabilities, throughput and spectrum utilization. Numerical results are presented to highlight the analysis. With numerical results, it is illustrated that the proposed strategy with the integration of queues and retry policy outperforms the existing ones without considering retrial transmission or queue support. In accordance, analytical results under the proposed strategy show significant improvements in terms of the throughput, forced termination and dropping probabilities. Results have also shown that the sensing errors remarkably influences the performance of CRNs by degrading SU and PU performance, which differs owing to their priority privileges. The incorporation of λ_{FAR} into the CTMC model allows obtaining exact and more accurate state transition probabilities, which, in turn, improves the calculation of the performance evaluation metrics.

Chapter 5

Dependability-Based Analysis in CRNs with Retrials and Channel Reservation

"*The most reliable way to predict the future is to create it.*"

— *Abraham Lincoln*

5.1 Introduction

The current research efforts on wireless communication systems have identified the need for large extent improvements in accessibility and reliability of communication services. Ultra-reliable communication (URC) and high data rate are two among essential service requirements in emerging 5G and beyond networks. As mentioned earlier, cognitive radio networks (CRNs) are envisaged as a promising solution for improving the quality of service (QoS) and ensuring URC in future networks. URC aims at achieving a certain level of communication service almost 100% of the time with higher degrees of reliability and availability of network resources in specific scenarios such as emergency management and traffic safety. However, achieving URC is a challenging task. Therefore, studying the availability and reliability aspects of CRNs from the perspective of dependability the-

This work has appeared in **Shruti and R. Kulshrestha, Computer Communications, Elsevier, 158 (2020) 51-63.** (https://doi.org/10.1016/j.comcom.2020.04.055)

ory is of vital importance to its successful operation in the near future, as discussed by Mendis et al. [235].

In contrast to other wireless networks, CRNs are more prone to channel access failures from the secondary user (SU) network's point of view. In general, channels in CRN could be unavailable for primary users (PUs) and SUs owing to two fundamental reasons, i.e. 1) for PUs if the spectrum is already occupied by other PUs and for SUs if the spectrum is already occupied by other PUs and/or SUs in the system; and 2) for both PUs and SUs if a channel itself fails due to software malfunctioning, hardware failure, channel fading, or shadowing. Various techniques have been proposed in the literature to improve the performance of CRNs (e.g., see Zhu et al. [236]; Khodadadi et al. [237]). However, therein, the main focus is merely by considering resource insufficiency due to traffic conditions. Due to the complexity of analysis, to date, little work has been done regarding the investigation of channel failures which can easily result in network performance degradation. To perform a realistic reliability analysis, it is thus required to consider performance changes that are associated with channel failures and repairs.

To support diverse services, in this chapter, a CRN is modeled which serves for both real-time SUs (RSUs) and elastic SUs (ESUs). With regard to the priority mechanism, PUs are always given the highest priority over SUs. For SUs, since RSUs are sensitive to transmission delay, they are given priority over ESUs to access the available channels once they are admitted in the network using spectrum handover. Accordingly, a channel reservation scheme is proposed to mitigate their forced terminations because of channel failures and insufficient resources. Moreover, RSUs are prioritized over ESUs in case of preemption upon PU arrival. Since prioritization may greatly hinder the communication of elastic traffic, the phenomenon of retrial transmission for leveraging the ESUs' performance is considered in this model. Furthermore, to find more practical network managerial insights, balking (refuse to join the retrial orbit) and reneging (leave the orbit after joining) phenomena of ESUs are also taken into account with the aim of investigating their impatient behavior. The main contributions of this work are highlighted as follows.